Supplemental Discussion

Infrared spectroscopy

We obtained near infrared reflectance spectra of 26 bright KBOs with NIRC, the near-infrared imaging spectrograph on the W.M. Keck Telescope using standard observational and data reduction methods[19]. The spectra cover from 1.4 to 2.4 μm with a spectral resolution $\lambda/\Delta\lambda \sim 160$ (see Supplemental Figure 1). The region between 1.81 and 1.89 μm has residual contamination by telluric H_2O lines, thus this region is masked out in the spectra. The KBO spectra were normalized to a relative reflectance of 1.0 by dividing each spectra by its median reflectance from 1.7 μm to 1.8 μm. This region is relatively flat in the NIR spectrum of water ice which is seen on some KBOs, thus KBOs with strong water ice features are scaled similarly to those with no water ice. Water ice has broad absorption features at 1.5 μm and 2.0 μm microns. To describe the absorption due to water ice in our spectra, we defined a quantity, A_w, as the fractional absorption at 2 μm. Specifically, we measured the fractional difference in the median reflectance between 1.7 μm to 1.8 μm and 2.0 μm to 2.1 μm. Error bars given for these measurements represent the 1σ uncertainties derived from the dispersions of the reflectance in the wavelength ranges. In addition to the spectra we obtained, we have made estimates of Aw for 1993 SC,1996 TO66, 1996 TL66, 1997 CS29, 2002 VE95, and Orcus, which have published spectra [4,20-24].

Colours

The V band through I band reflectance of KBOs can be well described by a single spectral gradient, G, that can be calculated from V,R, and I band photometric measurements[8]. We obtained visible colour measurements for 30 of the 32 total KBO spectra from published sources[3,8,25,26] and calculated the colour gradient and its uncertainty. The errors given for these measurements are 1σ uncertainties derived by propagating the uncertainties of the individual measurements. Five objects had no I-band measurements and one object had no R-band measurement. The spectral gradient was calculated for these objects using only the two available measurements. We find that the average difference in the gradient calculated using two versus three reflectance measurements is small, and therefore expect that the error introduced by using only a single colour measurement to be small compared to the errors in the colour measurements.

Orbital dynamics

Orbits of objects in the Kuiper belt precess and oscillate over time due to interactions with the giant planets. The instantaneous ("osculating") orbital elements are only a snapshot in time of these oscillating orbital elements. For objects with small eccentricities and inclinations the time-averaged orbital elements can be easily determined analytically, but for the higher inclination and eccentricity objects considered here we must resort to numerical techniques. Using the SWIFT orbital integration package[27], we integrate the orbits of each of the KBOs for a period of 50 Myr including only the gravitational influence of the sun and the four giant planets. We then take the average semimajor axis, eccentricity, and inclination over 50 Myr to be the proper elements. Five of the six KBOs have well behaved orbits which simply oscillate. 2003 EL61, in contrast, is found to be trapped within the 12:7 mean motion resonance with Neptune and thus exhibits large excursions in eccentricity even over the 50 Myr time period (see Supplemental Figure 2).

To examine whether 2003 EL61 could have originally been a member of the very tight central clump we randomly chose 32 objects with proper orbital elements within the semimajor axis range of 43.3 ±0.3 AU, the eccentricity range 0.12±0.025 and the inclination range 27.3±0.5 degrees and integrated their orbits forward 1.5 Gyr. Most objects exhibited stable behaviour like that of the majority of the known fragments. Five of the randomly selected objects, however, became trapped within the nearby 12:7 mean motion resonance (as 2003 EL61 currently is) and suffered an upward diffusion in eccentricity. Results of the orbital integrations are shown in Supplemental Figure 2.

doi: 10.1038/nature05619

Supplemental Figure

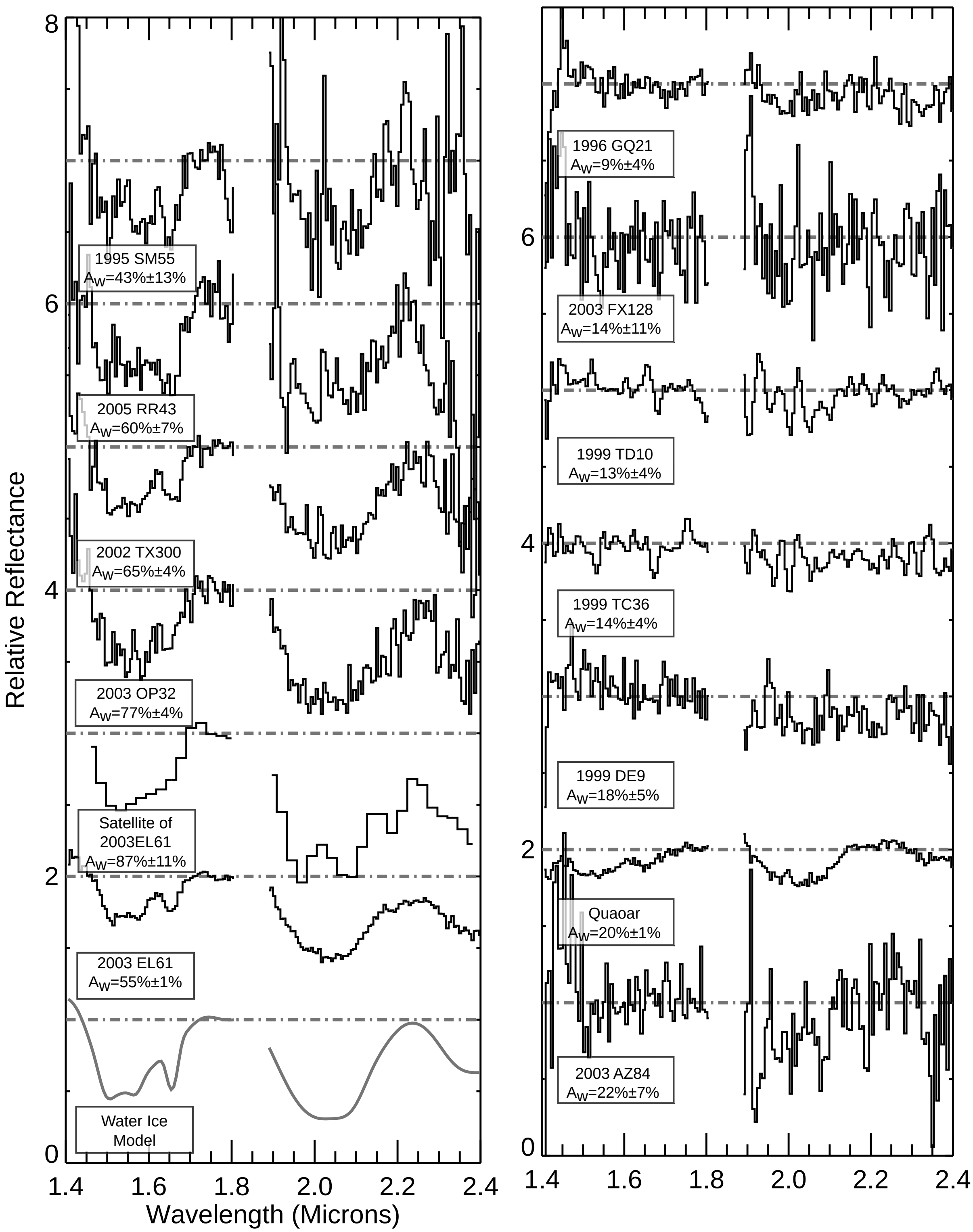

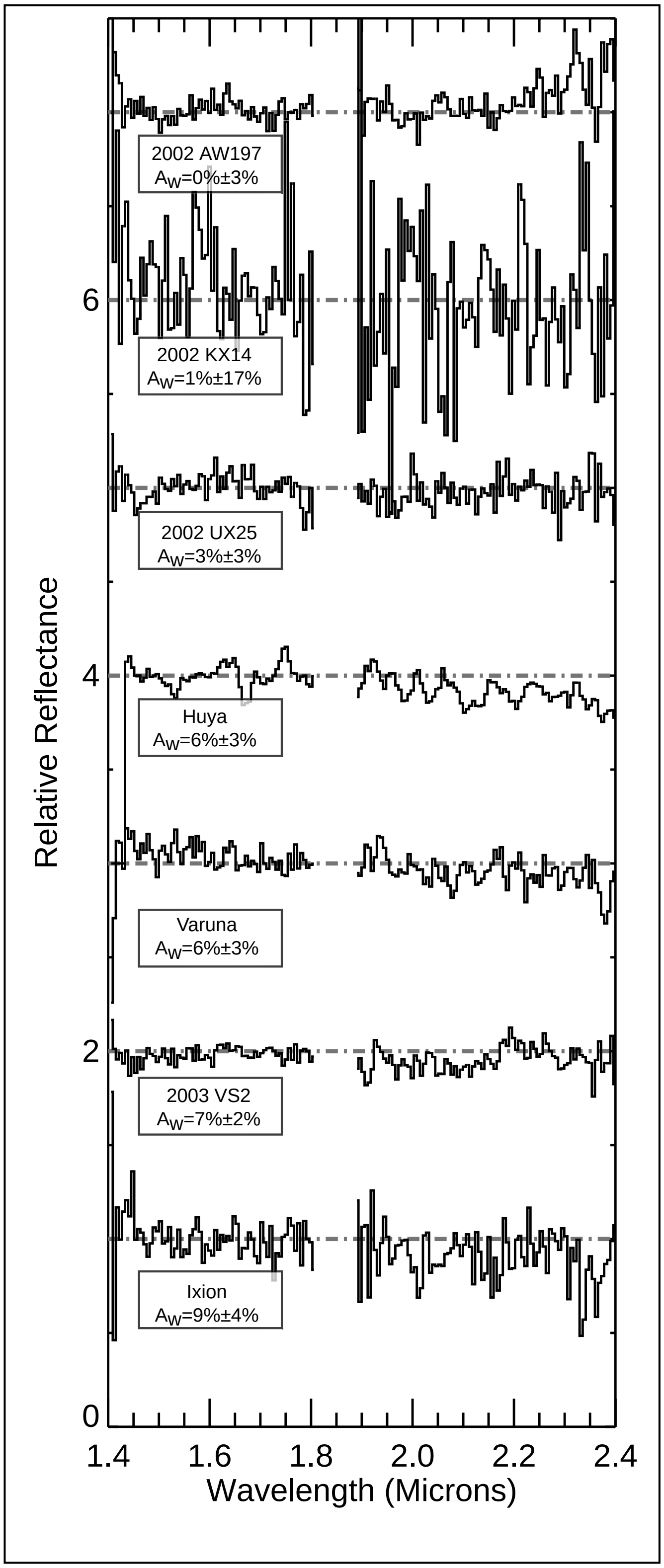
2002 AW197
AW=0%±3%
2002 KX14
AW=1%±17%
2002 UX25
AW=3%±3%
Huya
AW=6%±3%
Varuna
AW=6%±3%
2003 VS2
AW=7%±2%
Ixion
AW=9%±4%
Relative Reflectance
0
2
4
6
1.4
1.6
1.8
2.0
2.2
2.4
Wavelength (Microns)

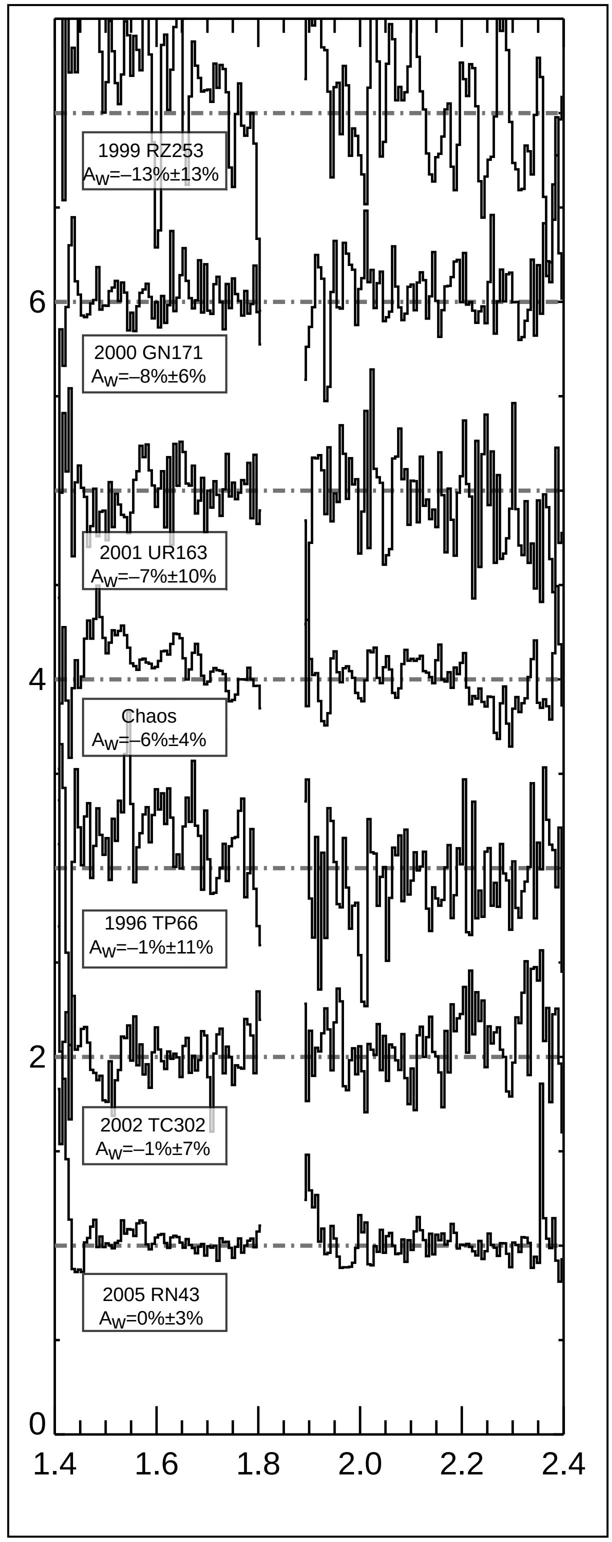
1999 RZ253
AW=–13%±13%
2000 GN171
AW=–8%±6%
2001 UR163
AW=–7%±10%
Chaos
AW=–6%±4%
1996 TP66
AW=–1%±11%
2002 TC302
AW=–1%±7%
2005 RN43
AW=0%±3%
0
2
4
6
1.4
1.6
1.8
2.0
2.2
2.4

Supplemental Figure 1: The reflectance spectra of 27 KBOs obtained with the Near Infrared Camera[28] on the W.M. Keck Telescopes. The spectra are normalized by the reflectance at 1.7 μm and are shifted by units of 1.0. The grey dashed lines mark the 0 and 100% relative reflectance for each spectrum. The first panel shows the spectra of 2003 EL61, its outer satellite[2] and the 5 fragments. A reflectance model of pure water ice is also shown (the smooth, dark grey line) for reference is also displayed in this panel. The model was created using a Hapke model and an ice temperature of 40K with a grain size of 50 μm[29,30]). The model shows the broad water ice absorptions at 1.5 and 2.0 μm that are also seen in the spectra of the fragments. A feature at 1.65 μm due to crystalline water ice feature is also seen in each of the KBOs with water ice spectra that has sufficient signal-to-noise. Previously published spectra of 1999 TO66 also shows similarly strong water ice features[31]. The strength of the water ice absorption for 2003 EL61 and the proposed fragments and the satellite are much stronger than is seen on the remaining.

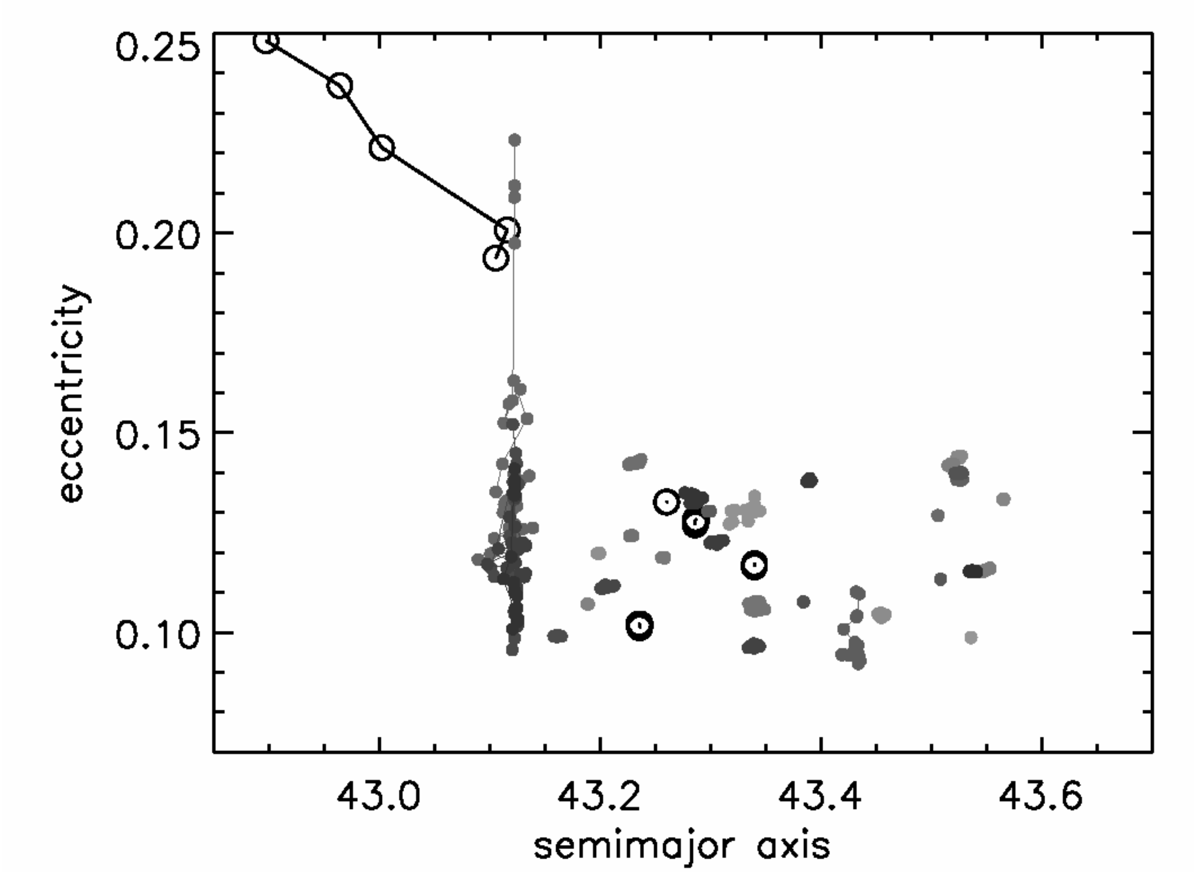

Supplemental Figure 2. Results of long term orbital integrations of the orbits of Kuiper belt objects in the vicinity of the collisionsal family. The large open circles show 50 Myr averages of the orbital elements of each of the members of the collisional family over the course of the 1.5 Gyr integration. The most eccentric member of the family is 2003 EL61, which has rapidly evolving orbital elements owing to its residence in the 12:7 mean motion resonance with Neptune. The small grey dots represent the orbital elements of 32 test particles randomly selected to have proper elements within the semimajor axis range of 43.3 ±0.3 AU, the eccentricity range 0.12±0.025 and the inclination range 27.3±0.5 degrees. Of these 32 test particles, 5 become trapped in the same 12:7 mean motion resonance as 2003 EL61 and suffer significant eccentricity diffusion.

Supplemental Table

Supplemental Table 1

Object	Absorption Depth(ref.)	Visible Gradient (ref.)	
2003 EL61	55 ±1	-0.18 ±0.67	(1)
S/2005 (2003 EL61) 1	87 ±11	NA	–
2003 OP32	77 ±4	-1.09 ±2.20	(Rab.)
1996 TO66	65 ±5 (2)	2.38 ±2.036	(10)
2002 TX300	65 ±4	0.00 ±0.67	(13)
2005 RR43	60 ±7	NA	–
1995 SM55	43 ±13	1.79 ±2.60	(10)
Orcus	22 ±4 (7, 4)	1.93 ±1.41	(11)
2003 AZ84	22 ±7	2.23 ±1.07	(12)
Quaoar	20 ±1	28.48 ±1.19	(12)
2002 VE95	20 ±4 (3)	38.81 ±2.59	(Teg.)
1999 DE9	18 ±5	20.74 ±3.08	(10)
1999 TC36	14 ±4	30.42 ±3.76	(Teg.)
1999 TD10	13 ±4	13.78 ±2.95	(10)
2003 FX128	14 ±11	20.64 ±3.39	(10)
1996 GQ21	9 ±3	38.05 ±5.04	(10)
Ixion	9 ±4	23.13 ±2.87	(10)
2003 VS2	7 ±2	20.64 ±2.26	(Teg.)
Varuna	6 ±3	27.86 ±4.30	(11)
Huya	6 ±3	24.51 ±6.02	(10)
2002 UX25	3 ±3	20.64 ±2.26	(Teg.)
2002 KX14	1 ±17	26.42 ±2.37	(Teg.)
2002 AW197	0 ±3	22.45 ±1.62	(11)
2005 RN43	0 ±3	NA	–
1996 TL66	0 ±8 (6)	3.02 ±3.65	(10)
1993 SC	0 ±10 (5)	37.75 ±7.13	(10)
1997 CS29	0 ±10 (8)	27.31 ±3.63	(10)
2002 TC302	-1 ±7	33.72 ±2.50	(10)
1996 TP66	-1 ±11	32.50 ±6.86	(10)
Chaos	-6 ±4	22.11 ±3.94	(11)
2001 UR163	-7 ±10	52.92 ±2.47	(Teg.)
2000 GN171	-8 ±6	26.13 ±3.99	(10)
1999 RZ253	-13 ±13	27.82 ±5.34	(10)

1. Rabinowitz, D.L. et al. Astrophysical Journal 639, 1238-1251 (2006). 2. Brown, R.H., Cruikshank, D.P. & Pendleton, Y. Astrophysical Journal 519, L101-L104 (1999). 3. Barucci, M.A., et. al. Astronomy & Astrophysics. 445, 725-730. (2006). 4. DeBergh, C. et. al. Astronomy & Astrophysics 437, 1115-1120 (2005). 5. Jewitt, D.C. & Luu, J.X. Astronomical Journal 122, 2099-2114 (2001). 6. Luu, J.X. & Jewitt,D.C. Astrophysical Journal 494, L117-L120 (1998). 7. Trujillo, C.A., et al.. Astrophysical Journal 627, 1057-1065 (2005). 8. Grundy, W.M., Buie, M.W. & Spencer, J.R. Astronomical Journal 130, 1299-1301 (2005). 9. Binzel, R.P. Science 241, 1070-1072 (1988). 10. Hainaut, O.R. & Delsanti. Astronomy & Astrophysics 389, 641-664 (2002). 11. Barucci, M.A., et al. Astronomical Journal 130, 1291-1298 (2005). 12. Fornasier, S. et al. Astronomy & Astrophysics 421, 353-363 (2004). 13. Doresoundiram, A. et al. Icarus, 174, 90-104 (2005) Teg. Tegler et al. In prep. See *http://www.physics.nau.edu/~tegler/research/survey.htm*

Supplemental Notes

References

19. Brown, M.E., Near infrared spectroscopy of Centaurs and irregular satellites. *Astron. J.* **119,** 977-983 (2000).
20. Jewitt, D.C., & Luu, J.X., Colors and spectra of Kuiper belt objects. *Astron. J.* **122,** 2099-2114 (2001).
21. Brown, R.H., Cruikshank, D.P. & Pendleton, Y. Water Ice on Kuiper Belt Object 1996 TO66. *Astrophys. J.* **519,** L101-L104 (1999).
22. Luu, J.X & Jewitt, D.C. Optical and infrared reflectance spectrum of Kuiper belt object 1996 TL66. *Astrophys. J.* **494,** L117-L120 (1998).
23. Trujillo, C.A., Brown, M.E., Rabinowitz, D.L. & Geballe, T.R. Near-Infrared surface properties of the two intrinsically brightest minor planets: (90377) Sedna and (90482) Orcus. *Astrophys. J.* **627,** 1057-1065 (2005).
24. de Bergh, C., Delsanti, A., Tozzi, G.P., Dotto, E., Doressoundiram, A. & Barucci, M.A., The surface of the transneptunian object 90482 Orcus. *Astron. & Astrophys.* **437,** 1115-1120 (2005).
25. Doressoundiram, A., Peixinho, N., Doucet, C., Mousis, O., Barucci, M.A., Petit, J.M. & Veillet, C. The Meudon Multicolor Survey (2MS) of Centaurs and trans-neptunian objects: extended dataset and status on the correlations reported. *Icarus* **174,** 90-104 (2005).

26. Delsanti, A., Hainaut, O., Jourdeuil, E., Meech, K.J., Boehnhardt, H. & Barrera, L. Simultaneous visible-near IR photometric study of Kuiper Belt Objects surfaces with the ESO/Very Large Telescopes. *Astron. & Astrophys.* **417,** 1145-1158 (2004).

27. Levison, H.F. & Duncan M.J. The long-term dynamical behavior of short-period comets. *Icarus* **108,** 18-36 (1994).

28. Matthews, K. & Soifer, B.T. The near infrared camera on the W.M. Keck telescope. *Experimental Astronomy* **3,** 77-84 (1994).

29. Hapke, B. Bidirectional reflectance spectroscopy 1. Theory. *J. of Geophys. Res.* **86,** 4571-4586 (1981).

30. Grundy, W.M. & Schmitt, B. The temperature-dependent near-infrared absorption spectrum of hexagonal H2O ice. *J. of Geophys. Res.* **103,** 25809-25822 (1998).